Supplemental Materials, Hunt et al., submitted.

Table S1. Genes Upregulated in *Mtg16*$^{-/-}$ LSK and Repressed in E47ER Hematopoietic Progenitor Cells

Asb7	Dntt	Hip1	Myom1
Calcrl	Entpd4	Il18r1	Phf7
Ccl3	Fmn2	Itga6	Sytl4
Ctla2a	Gcnt2	Loxhd1	Tex15
Dlk1	Gem	Lypla3	

Table S2. Genes Upregulated in Both *Mtg16*$^{-/-}$ LSK and OP9-DL1/E47ER Hematopoietic Progenitor Cells

Arhgef3	Gadd45b	Kif5a	Rassf4
Atp13a2	Galnt2	Ltb	Rps6ka6
Atp2a3	Gata3	Map3k8	Sgsh
CD52	Hcls1	Nnt	Sla
CD80	Hemgn	Nox4	Slc45a4
Celsr1	Hes1	Olfml1	Slco4a1
Csf2rb2	Hsd11d1	P2ry14	Smad7
Ctsl	Id2	Pcmtd2	Socs3
Dcx	Il10ra	Pik3cd	Tcf7l2
Esr1	Il1r1	Plaur	Tcrb-V13
Fyn	Itgam	Ptprc	Tle6

Table S3. Genes Upregulated in *Mtg16*$^{-/-}$ LSK and Repressed in E47ER 1F9 Thymoma Cells

Adarb1	Gata3	Mbl1	Rasgef1b
Brd8	Gem	Mdga1	Rgs1
Cav2	Hhex	Myom1	Slc16a9
Col18a1	Hivep3	Nrxn1	Tex15
Dlk1	Hoxb2	Pik3r1	Ttr
Dusp18	Lonrf3	Plaur	Xlr3a

Table S4. Genes Upregulated in *Mtg16*$^{-/-}$ LSK and Activated in E47ER 1F9 Thymoma Cells

Bcl2l1	Galnt2	Irf6	Sytl4
Ctsl	Gimap6	Itga6	Tcfec
Cyfip2	Hemgn	Itpr3	Tle6
Dhx9	Hes1	Jag2	Tmem35
Ebi3	Id1	Mxd4	Tnfrsf22
Efhc2	Id2	Nnt	Tnfrsf23
Esr1	Il10ra	Nsg2	Vegfa
Gadd45b	Il21r	Socs3	Wfdc2

Figure S1. Increased development of myeloid lineages in the *Mtg16*$^{-/-}$ mouse. (A) Increased production of Gr1^{+}/Mac1^{+} cells in *Mtg16*$^{-/-}$ bone marrow, both as a percentage of total cells and as an absolute number in 2 hind limbs (both femur and tibia). An unpaired, two-tailed t-test shows * $p<0.05$, *** $p<0.001$. Shown are data from a representative experiment from one of two independent experiments performed with 3 mice of each genotype, for a total N=7 mice. (B) Increased population of Gr1^{+}/Mac1^{+} cells in *Mtg16*$^{-/-}$ spleens shown both as a percentage of total cells and as an absolute number per spleen. An unpaired, two-tailed t-test shows ** $p<0.01$. N=3. Shown are data from a representative experiment from one of two independent experiments, for a total N=7 mice.

Figure S2. Analysis of the *Mtg16*-null thymus. (A) Left panel shows a photo of a representative thymus from a 6-8 week old wild type and *Mtg16*-null mouse. The right panel shows a graph of the average of the total numbers of WT and *Mtg16*-null thymocytes, +/- standard deviation (SD). An unpaired, two-tailed t-test shows ** $p<0.01$. Shown are data from a representative experiment with 5 mice of each genotype, with a total N=17. (B) Left panels show flow cytometric plots of CD4 and CD8 expression in the WT and *Mtg16*-null thymus. Graphs in the right panels depict both the average percentage of total thymocyte number (top) and the average absolute cell number (bottom) in each population, +/- SD. Shown are data from a representative experiment with 5 mice of each genotype, with a total N=17. An unpaired, two-tailed t-test shows * $p<0.05$, ** $p<0.01$, ***$p<0.001$ (C) Flow cytometric analysis of CD4^{-}CD8^{-} thymocytes for expression of CD44 and CD25 of the double negative population shown in B. Graphs depict both the average of the percentage of total CD4^{-}CD8^{-} number (top) and the absolute cell number (bottom) in each population, +/- SD. Shown are data from a representative

experiment with 5 mice of each genotype, with a total N=17. An unpaired, two-tailed t-test shows * $p<0.05$, ** $p<0.01$, ***$p<0.001$. For (A-C) a minimum of three independent experiments were performed with at least three pairs of age-matched WT and Null mice.

Figure S3. Relative expression of *Mtg* family members across murine hematopoiesis. Graphs show the relative levels of *Mtg16*, *Mtg8*, and *Mtgr1* in various hematopoietic populations. The indicated populations were isolated by flow cytometry and the mRNA levels determined using qRT-PCR. For each population, at least two independent samples were collected and analyzed in duplicate. The average expression is shown +/- SD, relative to the value in Lineage negative bone marrow.

Figure S4. *Mtg16*$^{-/-}$ DN2 thymocytes cultured on OP9-DL1 stroma exhibit growth defects. (A) Growth curves for DN2 cells cultured on OP9-DL1 stroma as assessed by cell counts. Shown are data from a representative experiment from one of three independent experiments performed with 2-3 mice of each genotype, for a total N=7 mice. (B) Representative flow cytometry plots of DN2 cells assessed for DNA content using propidium iodide staining of day 7 OP9-DL1 cultures. Lower panel shows a quantitative assessment of this analysis. Shown are data from a representative experiment from one of two independent experiments performed with 3 mice of each genotype, for a total N=6 mice. (C) Annexin V staining of Day 7 OP9-DL1 cultures from DN2 cells. Shown are data from a representative experiment from one of two independent experiments performed with 3 mice of each genotype, for a total N=6 mice.

Figure S5. Expression of MSCV-*myc-Mtg16*-GFP mutant proteins. Immunoblot analysis is shown of cell lysates expressing the indicated proteins using anti-c-Myc.

Figure S6. Mtg16 associates with E47 and the Notch Intracellular Domain. (A) Mtg16 F210A retains binding to E47 by co-immunoprecipitation. The indicated proteins were co-expressed and association measured by immunoprecipitation followed by western blot analysis. Positions of molecular weight markers are indicated to the right. (B) Deletion of NHR1 is not sufficient to remove the interaction between Mtg16 and E47. The indicated proteins were co-expressed and association measured by immunoprecipitation (IP) followed by western blot analysis (WB). Positions of molecular weight markers are indicated to the right. (C) Mtg16 F210A and R220A retain associating with the Notch1-Intracellular Domain by co-immunoprecipitation, while the ΔNICD no longer binds. The indicated proteins were co-expressed and association measured by immunoprecipitation (IP) followed by western blot analysis (WB). Positions of molecular weight markers are indicated to the right. (D) F210A, R220A, and ΔNICD do not affect Mtg16-dependent repression. Mtg16 and the indicated mutants were fused in frame with the GAL4 DNA binding domain and tested for repression using a Gal4-luciferase reporter construct. Graph shows the average relative luciferase values from an Gal4 reporter plasmid co-transfected with vector control or the indicated Mtg16 or mutant thereof. The values were normalized to a renilla-luciferase plasmid to control for specificity and transfection efficiency. The experiment was performed twice in triplicate.

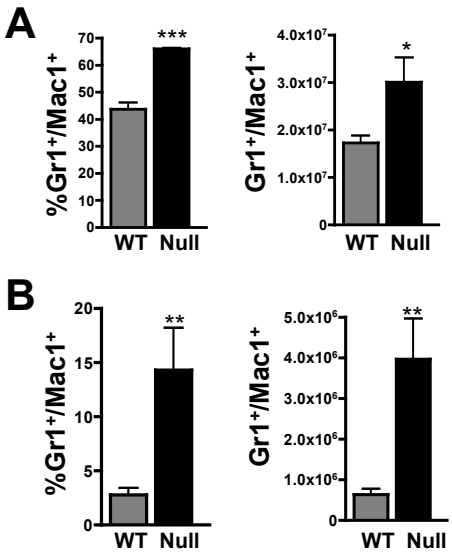
A
%Gr1+/Mac1+
70
60
50
40
30
20
10
0
***
WT
Null
Gr1+/Mac1+
4.0x10^7
3.0x10^7
2.0x10^7
1.0x10^7
0
*
WT
Null
B
%Gr1+/Mac1+
20
15
10
5
0
**
WT
Null
Gr1+/Mac1+
5.0x10^6
4.0x10^6
3.0x10^6
2.0x10^6
1.0x10^6
0
**
WT
Null

Figure S1

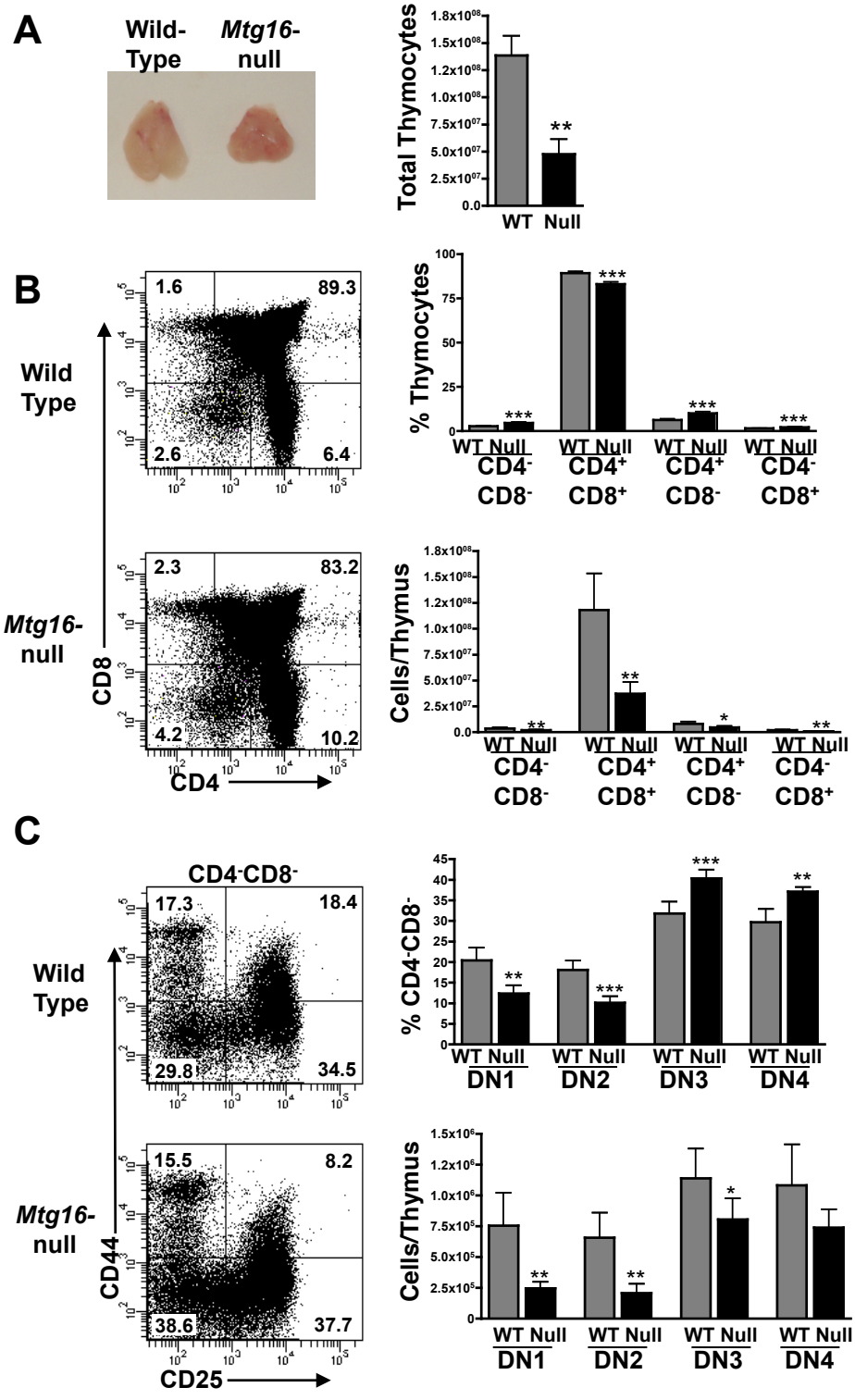
A
Wild-Type
Mtg16-null
Total Thymocytes
WT Null
B
Wild Type
Mtg16-null
CD8
CD4
1.6
89.3
2.6
6.4
2.3
83.2
4.2
10.2
% Thymocytes
Cells/Thymus
CD4- CD8-
CD4+ CD8+
CD4+ CD8-
CD4- CD8+
C
CD4-CD8-
17.3
18.4
29.8
34.5
15.5
8.2
38.6
37.7
CD44
CD25
% CD4-CD8-
DN1
DN2
DN3
DN4

Figure S2

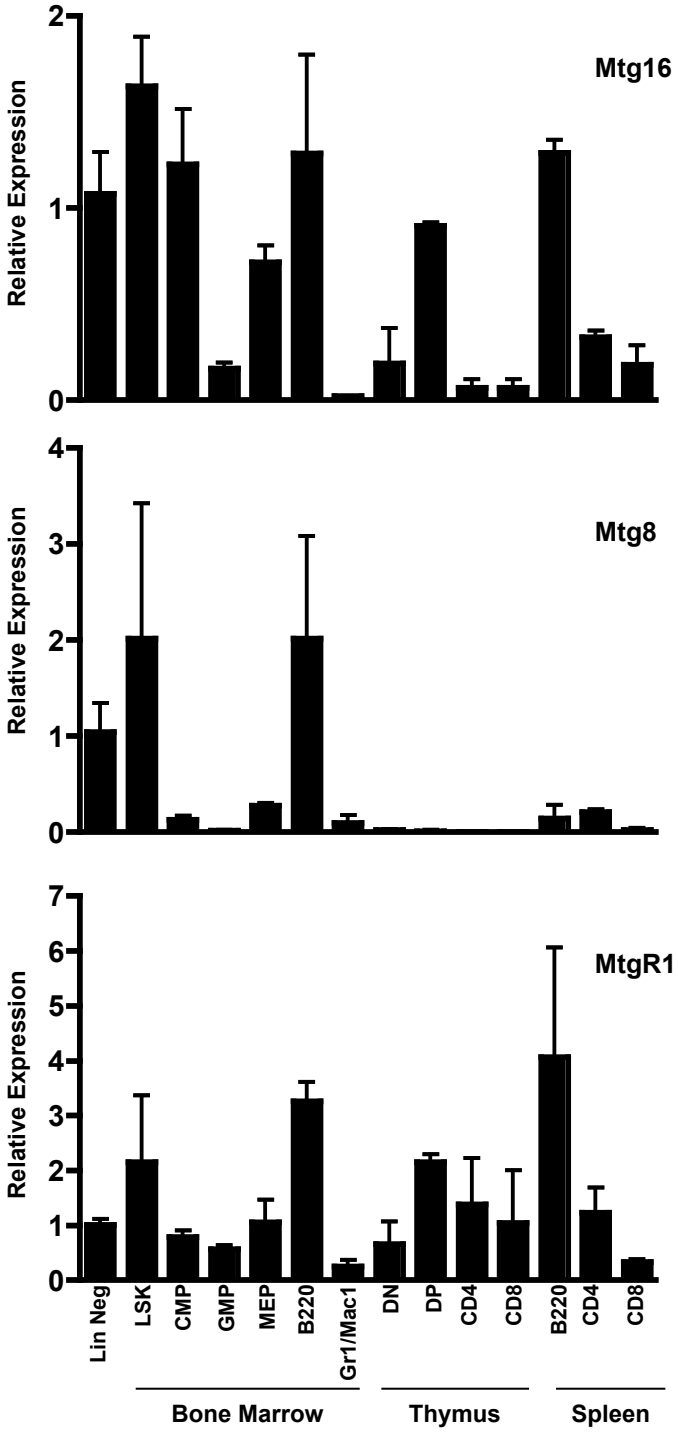
Mtg16
Relative Expression
2
1
0
Mtg8
Relative Expression
4
3
2
1
0
MtgR1
Relative Expression
7
6
5
4
3
2
1
0
Lin Neg
LSK
CMP
GMP
MEP
B220
Gr1/Mac1
DN
DP
CD4
CD8
B220
CD4
CD8
Bone Marrow
Thymus
Spleen

Figure S3

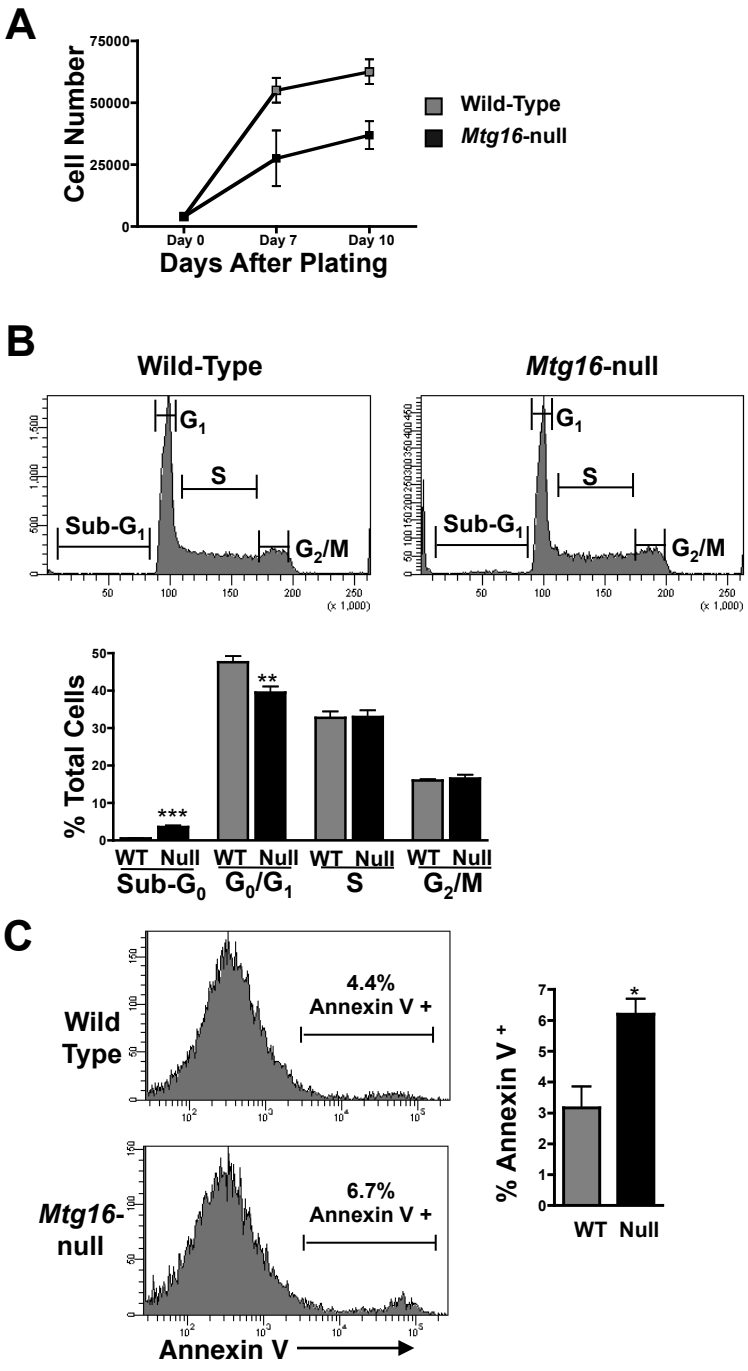
A
Cell Number
75000
50000
25000
0
Day 0
Day 7
Day 10
Days After Plating
Wild-Type
Mtg16-null
B
Wild-Type
Mtg16-null
G1
S
Sub-G1
G2/M
(x 1,000)
% Total Cells
***
**
WT Null
Sub-G0
G0/G1
S
G2/M
C
Wild Type
4.4%
Annexin V +
Mtg16-null
6.7%
Annexin V +
Annexin V
% Annexin V +
*
WT Null

Figure S4

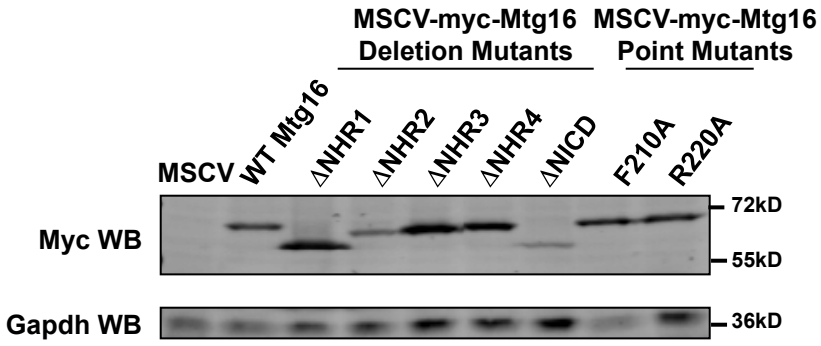
MSCV-myc-Mtg16
Deletion Mutants
MSCV-myc-Mtg16
Point Mutants
MSCV
WT Mtg16
ΔNHR1
ΔNHR2
ΔNHR3
ΔNHR4
ΔNICD
F210A
R220A
Myc WB
72kD
55kD
Gapdh WB
36kD

Figure S5

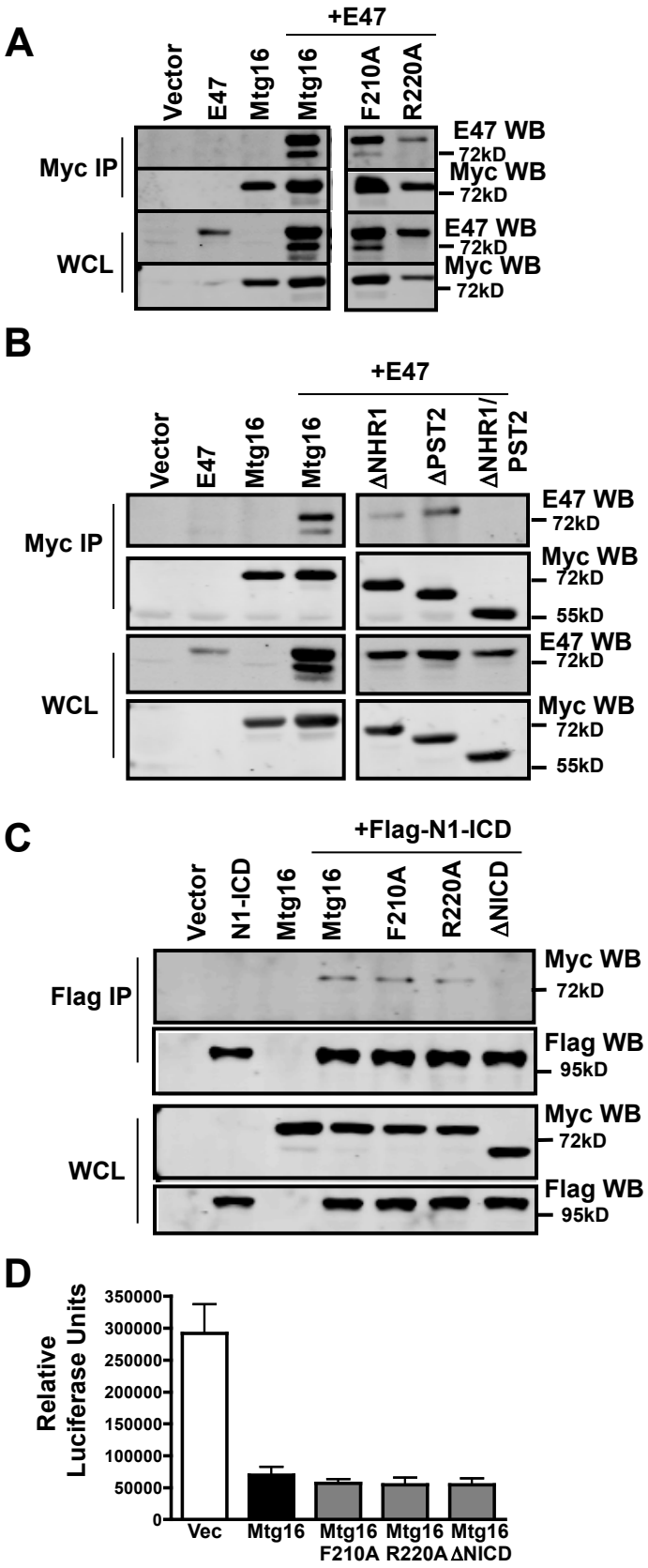
A
+E47
Vector
E47
Mtg16
Mtg16
F210A
R220A
Myc IP
WCL
E47 WB
72kD
Myc WB
72kD
E47 WB
72kD
Myc WB
72kD
B
+E47
Vector
E47
Mtg16
Mtg16
ΔNHR1
ΔPST2
ΔNHR1/
PST2
Myc IP
WCL
E47 WB
72kD
Myc WB
72kD
55kD
E47 WB
72kD
Myc WB
72kD
55kD
C
+Flag-N1-ICD
Vector
N1-ICD
Mtg16
Mtg16
F210A
R220A
ΔNICD
Flag IP
WCL
Myc WB
72kD
Flag WB
95kD
Myc WB
72kD
Flag WB
95kD
D
Relative
Luciferase Units
350000
300000
250000
200000
150000
100000
50000
0
Vec
Mtg16
Mtg16
F210A
Mtg16
R220A
Mtg16
ΔNICD

Figure S6